INTRODUCTION

Electrochemical reduction of CO_2 and/or H_2O to produce CO and/or H_2 could provide the basis of large-scale energy storage to smooth the dynamics of renewable power sources and electrical power demands (Figure 1), and if operated with renewable power sources, could mitigate CO_2 emissions from e.g. steel and cement production.

Micro-tubular solid oxide electrolysers and fuel cells are robust to thermal cycling, have fast start-up, facile to seal [3,4], and their volumetric power densities ($\propto \pi/d$) increase with decreasing tube diameter (d), so exceeding the values for planar structures.

Figure 1: Seasonal (daily average) and weekly (real daily variation) UK power demand for 2010 [1, 2].

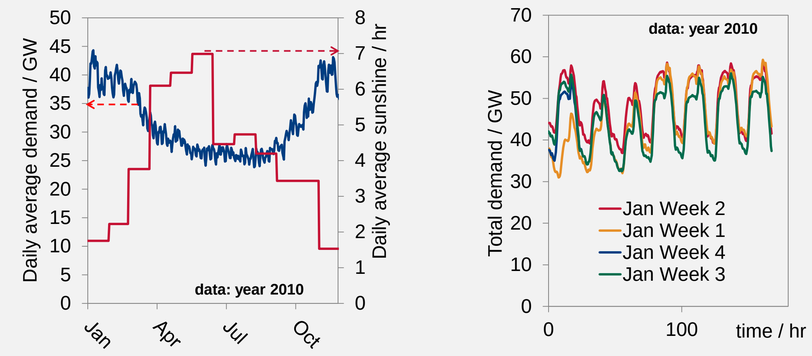

SOLID OXIDE ELECTROLYSER REACTIONS

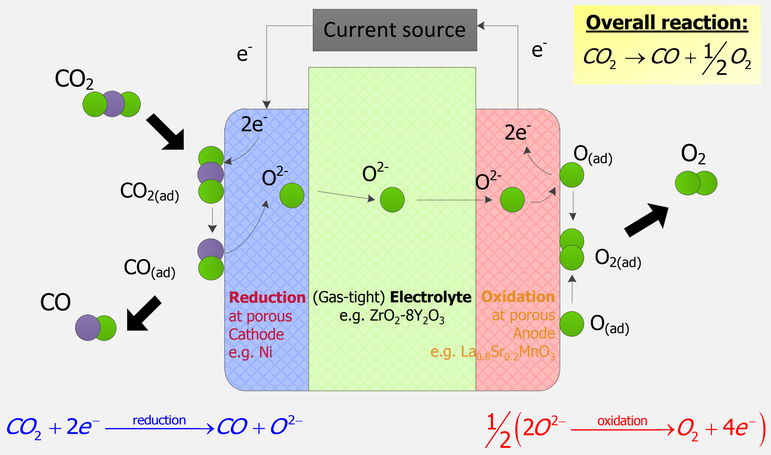

Figure 2: Schematic of electrolyser with oxide ion-conducting membrane operating at 700-800 °C. Working principles explained for CO_2 reduction.

Reactor fabrication

Electrolysers of the form Ni-YSZ|YSZ|YSZ-LSM|LSM (Figure 3) were prepared in two-steps (with YSZ = 8 Y_2O_3-ZrO_2 and LSM = $La_{0.8}Sr_{0.2}MnO_3$):

- Dual-layer co-extrusion phase inversion to produce Ni-YSZ|YSZ hollow fibre precursors (co-sintered at 1500 °C – 10 hours)
- Brush-coating of LSM-YSZ|YSZ layers followed (sintered at 1100 °C – 3 hours).

Figure 3: Reactor geometry

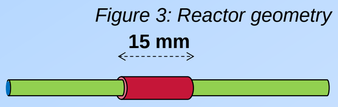

Figure 4: Phase inversion system to fabricate dual-layer hollow fibre precursors.

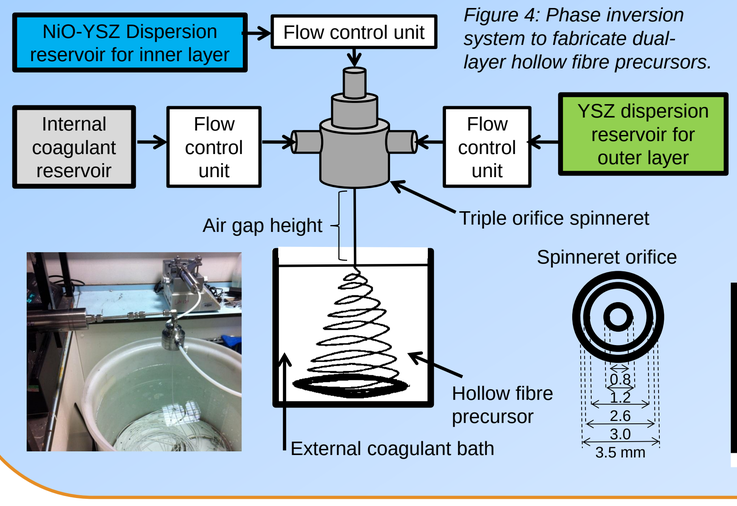

Fibre characterization

Electrolyte thicknesses between 19 (± 2) – 49 (± 3) µm have been achieved (Figure 5) and homogeneity within the different layers confirmed using energy-dispersive spectrometry (EDS) - Figure 6.

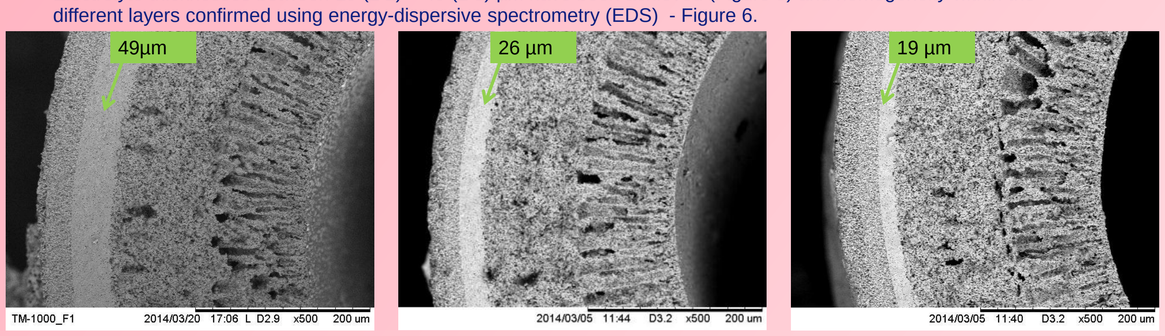

Figure 5: Scanning electron micrographs of (reduced) cross-sectioned fibres (post-operation) with varying electrolyte thickness.

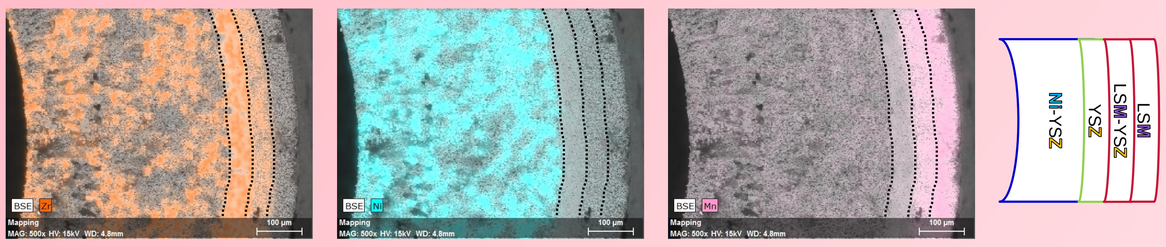

Figure 6: EDS maps of representative elements of the individual layers within the Ni-YSZ|YSZ|LSM-YSZ|YSZ electrolyser.

Porosities increased following reduction in an hydrogen atmosphere, which corresponded to the 41 % molar volume change between NiO and Ni. Inherent porosities within the un-reduced fibres were associated with the finger-like pores.

Figure 8 shows the change in pore size distribution, again confirming the formation of a sponge-type porosity in the bulk Ni-YSZ electrode contrasting with finger-like pores formed during phase inversion.

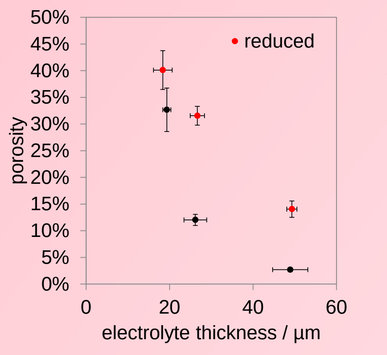

Figure 7: Porosity of (un)reduced fibres as a function of electrolyte thickness.

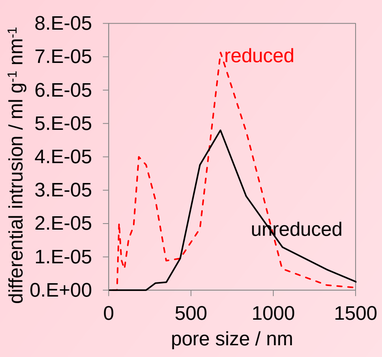

Figure 8: Pore size distribution of (un)reduced fibre (19 µm electrolyte).

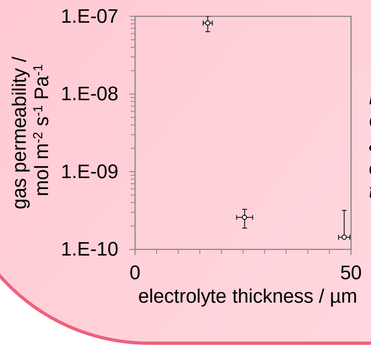

Figure 9: Gas-tightness as a function of electrolyte thickness.

Gas permeabilities decreased with increasing electrolyte thickness, approaching the gas-tightness benchmark of 10^{-10} mol m^{-2} s^{-1} Pa^{-1} set by Tan et al. [5].

Bending strength of the fibres was ca. 160 MPa for the 19 and 26 µm and 110 MPa for the 49 µm thick electrolyte fibres. This is due to the difference in shrinkage behaviour between YSZ and NiO-YSZ observed during sintering (quantitatively assessed using dilatometry).

Electrolysis performance: CO_2 reduction

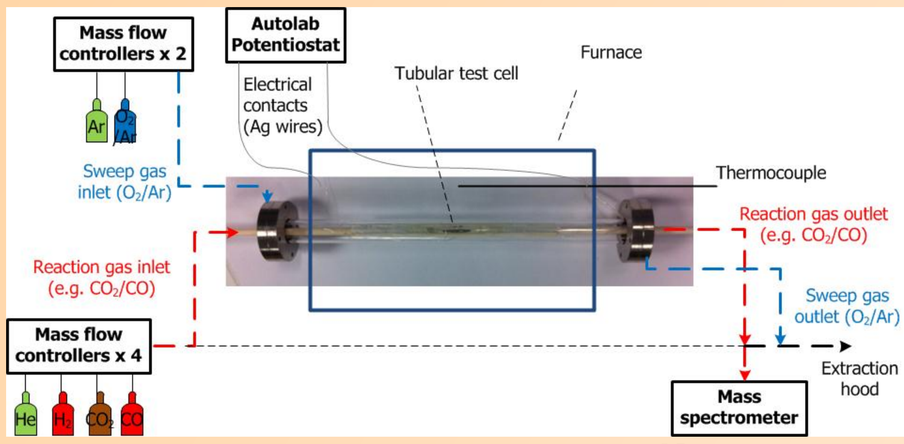

Figure 10: Schematic of experimental equipment .

Increasing operating temperature and decreasing electrolyte thickness enhanced electrolyser performance. (Figure 12). Temperature both increases electrolyte conductivities (1.9 to 4.3 S m-1 for 700-800 °C, respectively [6]) and enhances electrode kinetics.

Analysis of the ohmic resistance, based on impedance spectroscopy (Figure 11), revealed that electrolyte resistance contributed only 28-5% (50-15 µm / 700-800 °C) towards the total, the remaining losses being associated with the wires (⅓) and contact losses (⅔).

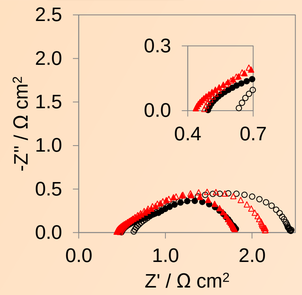

Figure 11: Electrical impedance spectra at 700 °C (unfilled) and 800 ºC (filled) for electrolyte thickness extremes: 15 (▲) and 50 (●) µm measured at open circuit potential difference.

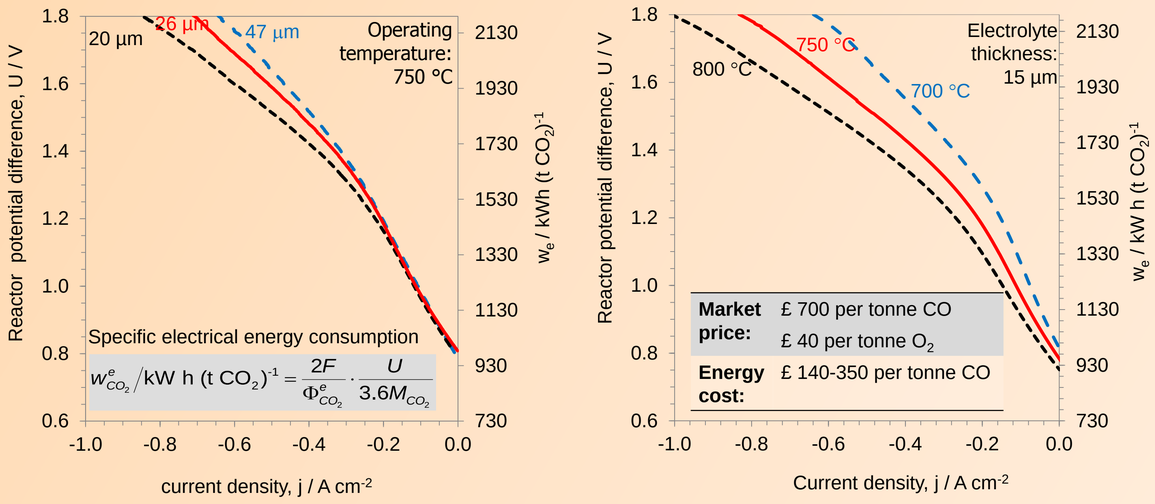

Figure 12: Effects of applied current density (j) and operating temperature/ electrolyte thickness on cell potential difference (U) and specific electrical energy consumption (w_e) at 90/10 CO_2/CO gas feed composition.

Product gases were analysed with on-line mass spectrometry, confirming 100% charge yield for steady state constant reactor potential difference experiments. Figure 13 shows the variation in reactant and product gas fluxes, following the effect of varying applied potential.

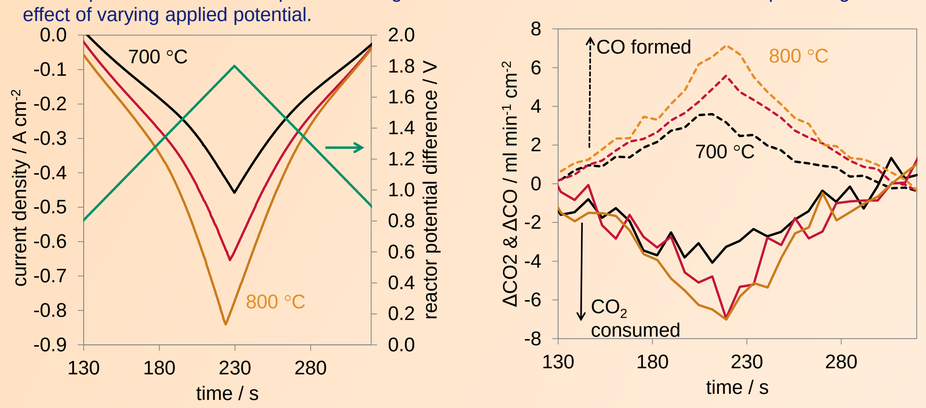

Figure 13: Effects of applied potential difference and operating temperature on current density (j) and resulting gas fluxes.

At 0.3 A cm^{-2} over ca. 10 hours, reactor potential differences increased by 2 mV hr^{-1}.

Reversibility of operating the solid oxide reactor in electrolyser (energy storage) and fuel cell (power re-generation) mode was demonstrated.

Electrolysis performance: CO_2 vs. H_2O reduction

Electrolyser performance was assessed as a function of feed-gas composition. Figure 14 shows that steam and (CO_2-H_2O) co-electrolysis performed similarly, depending on temperature being 58-68% better than CO_2/CO electrolysis. Hence it is likely, that the CO_2 reduction observed during co-electrolysis was mainly via the water-gas shift reaction ($CO_2 + H_2 \rightleftharpoons CO + H_2O$) rather than direct electrochemical reduction.

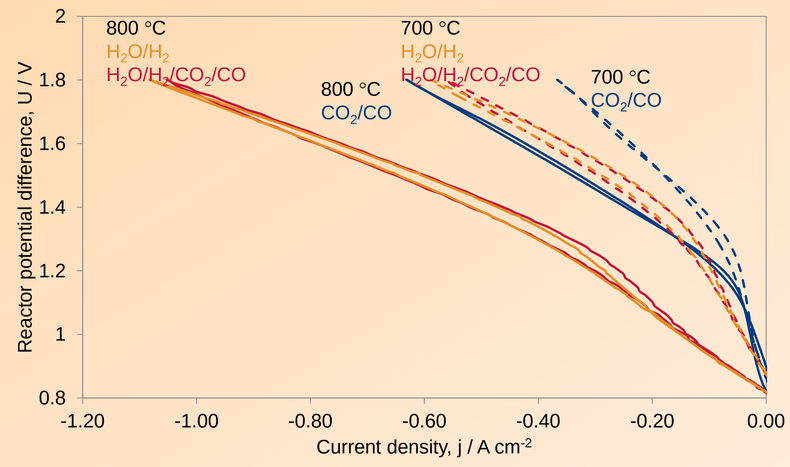

Figure 14: Effects of applied current density (j) and operating temperature on cell potential difference (U) for a 29 µm thick electrolyte at different reactant gas feed compositions:

- *90/10 CO_2/CO,*
- *40/10/40/10 CO_2/CO/H_2O/H_2*
- *90/10 H_2O/H_2*

Note: 56% of the reactant gas composition was He due to the total flow-rate requirements of the steam generator.

ACKNOWLEDGEMENTS & REFERENCES

- Financial support from the UK Engineering and Physical Sciences Research Council (EPSRC).

[1] Met Office: http://www.metoffice.gov.uk/climate/uk/2010/ [accessed June 2014].
[2] National Grid: http://www2.nationalgrid.com/uk/industry-information/Electricity-transmission-operational-data/Data-Explorer/ [accessed June 2014]
[3] K. Kendall, Int. J. Appl. Ceram. Technol., 2010, 7, 1.
[4] Y.Du, N.M. Sammes, J. Power Sources, 2004, 136, 66.
[5] X. Tan, Y. Liu and K. Li, AIChE J., 2005, 51, 1991.
[6] H. Zhu, R.J. Kee, J. Power Sources, 2003, 117, 61.

SUMMARY & FUTURE WORK

- Successful fabrication of Ni-YSZ|YSZ|LSM-YSZ|YSZ micro-tubular electrolysers using dual-layer phase inversion and sintering
- Maximum performance of 1.0 A cm^{-2} at 1.8 V in CO_2 electrolysis mode for 15 µm thick electrolyte
- Up to 68 % (800 °C) performance enhancement for H_2O and co-electrolysis compared with reduction of CO_2 alone.
- Wires (21-31 %) and contact losses (51-64 %), rather than the electrolyte itself (28-5%) were major contributors to ohmic losses
- Reactors can be operated reversibly (electrolyser and fuel cell mode)
- Ways to minimize the contact losses and long-term degradation are currently being investigated.